Electromagnetically excited audible noise in electrical machines

Kay Hameyer, François Henrotte & Koen Delaere
Katholieke Universiteit Leuven, E.E. Dept. ESAT / ELECTA
Kasteelpark Arenberg 10, B-3001 Leuven-Heverlee
E-mail: Kay.Hameyer@esat.kuleuven.ac.be

***Abstract* – With the rising utilisation of electrical machines to increase the output-power of the device several problems occur. Next to probable additional losses and other parasitic effects, aspects concerning the audible noise radiated by the device are of particular interest.**

This contribution is intended to give an overview to the problematic of the analysis of vibrations and audible noise radiated by electrical machines. It is not the intention of the authors to set off a scientific firework with various complicated equations in this contribution. The paper should rather give an insight in a complicated technical matter and should help to understand the mechanism of vibration and parasitic noise generation in electrical machines.

Rotating machines, such as the induction motor as well as non-rotating electrical machines, such as inductors or transformers are studied.

The origin of vibrations leading to noise radiations is studied and discussed to illustrate the way in which the analysis of the governing effects can be performed.

Magnetically generated radial pullout force waves in rotating electrical machines are the main cause of the excited audible noise, whereas magnetostriction plays an important role in transformers.

I. INTRODUCTION

Next to the audible noise generated by the ventilation and bearings of a rotating electrical machine, electromagnetically excited vibrations are a substantial cause of the overall audible noise radiated by the device. The present-day analytical knowledge for the analysis of magnetically excited noise was build up by Jordan [1, 2]. In this model e.g. for the induction machine, it is assumed that the stator of the machine can be represented by a thin ring, which is excited by radial forces. Such forces are determined from the interaction of the machine's fundamental field together with the harmonics in the air gap field. By employing computers for this analysis, relative quick results can be obtained. However, by using the idea of a simple ring provides only a limited model for the noise analysis, e.g. the influence of the stator teeth on the vibration behaviour of the stator lamination cannot be considered. The coupling between the winding and the stator, respectively the stator and the housing of the machine is not modelled in this approach. There is and has been a lot of research to study such couplings, which lead to the application of numerical models to enhance the degree of details modelled.

Modern and fast computers allow a numerical model of the analysis of such effects. A coupled electromagnetic field / structural dynamic problem can be defined and solved. The modelling and solution of such a numerical approach require huge computation times and is therefore not well suited for the day-by-day engineering task but provides in contrast to the analytical approach a very detailed picture of the problem under study. Various examples of numerical models can be found in the literature [3, 4, 5, 6]. As a starting point for the interested reader it is referred to the various technical papers authored by [3, 4, 5, 6], which are published in English language in international journals and presented on several international conferences.

II. AUDIBLE NOISE EXCITED BY ELECTRICAL MACHINES

The audible noise of rotating electrical machine can roughly been distinguished into some ventilation, bearing and electromagnetically caused noise. The ventilation noise is characterized in a broad-band frequency band of about 500… 1000 Hz. The bearings radiate audible noise of single-tones of frequencies larger 3 kHz. Due to the high sensitivity of the human ear at frequencies of 500… 3500 Hz, the magnetically excited vibrations in this frequency range are the most important ones. To restrict the analysis efforts analytical models are therefore usually limited to this frequency range and will be the ones treated in this paper. Key for the analysis of acoustic noise of electric machines is obviously the excitation of the stator vibrations and therefore the careful analysis of electromagnetic forces acting on the machine's body (Fig. 1).

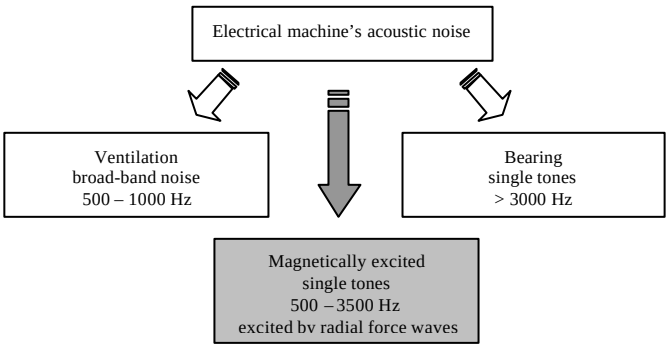

Fig. 1. Main sources of the acoustic noise in electrical machines.

To evaluate the sound noise of e.g. electrical machines particular definitions have to be done. Such definitions influence and constrain the model for the analysis. In Fig. 2 a room with a noise source and an observer at position 0 can be seen. The area around the source the immediate vicinity of the

source is called “near field”. When the observer is in this distance to the source the observed noise is determined by the geometrical details of the surface of the noise source. Being in the distance of the “far field”, geometrical details are not significant for the observed noise field. Therefore, the model of the source can be simplified and be assumed to be a point source without any geometrical outer dimension. This is the interesting distance for this study. Close to walls reflections become significant.

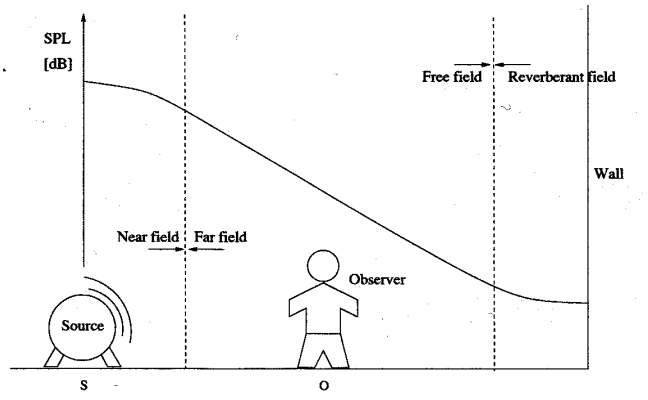

Fig. 2. Noise field definitions.

III. Analytic Induction Machine Noise Analysis

It was mentioned earlier, that the analytical motor model assumes to represent the stator lamination as a stiff and thin ring with particular mechanic and magnetic properties to guide the magnetic flux in the machine. Furthermore a not-slotted stator is assumed and that the iron is with an ideal permeability $\mu_{Fe} \to \infty$ [1]. Under these assumptions, the magnetic field lines leave the iron perpendicular to its surface and the surface stress is perpendicular to the iron surface as well. In cylindrical machines this radial force waves can excite the stator package to vibrate and therefore to radiate audible noise. The radial stress can be determined by:

$$\sigma_r(x,t) = \frac{b_d^2(x,t)}{2\mu_0} \tag{1}$$

x is the local stator coordinate, t the time and μ_0 the permeability of the free space. $b_d(x,t)$ represents the resulting air gap flux density, which is determined by the fields excited by the currents in the stator winding and rotor bars (Fig. 3). The stator as well as the rotor field has various field harmonics. Assuming rotary fields with the pole pair number ν:

$$b_n(x,t) = B_n \cos(\nu x - \omega_n t - \varphi_n), \tag{2}$$

and the approximation for the combination of two field waves in eq. (3) illustrates that two field waves already generate four radial stress waves. Remarkable in eq.(3) are the generated waves with the pole pair numbers $r = \nu_2 \pm \nu_1$ with the frequencies of $f_r = \frac{1}{2\pi}(\omega_{n2} \pm \omega_{n1})$. Due to their local distribution at the surface of the stator bore they excite the lamination to vibrate in particular modes (Fig. 4).

$$\begin{aligned}\sigma_r(x,t) = {} & \frac{B_{n1}^2}{4\mu_0}\cdot\{1+\cos(2\nu_1 x - 2\omega_n t - 2\varphi_{n1})\} \\ & + \frac{B_{n2}^2}{4\mu_0}\cdot\{1+\cos(2\nu_2 x - 2\omega_{n2} t - 2\varphi_{n2})\} \\ & + \ldots \\ & \frac{B_{n1}\cdot B_{n2}}{2\mu_0}\cdot\cos\{(\nu_2 \pm \nu_1)x - (\omega_{n2} \pm \omega_{n1})t - (\varphi_{n2} \pm \varphi_{n1})\} \\ & + \ldots .\end{aligned} \tag{3}$$

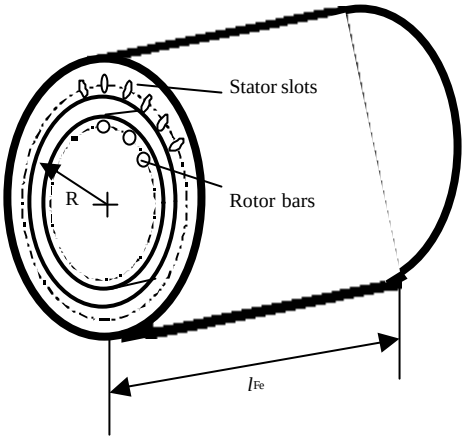

Fig. 3. Construction principle of an induction machine.

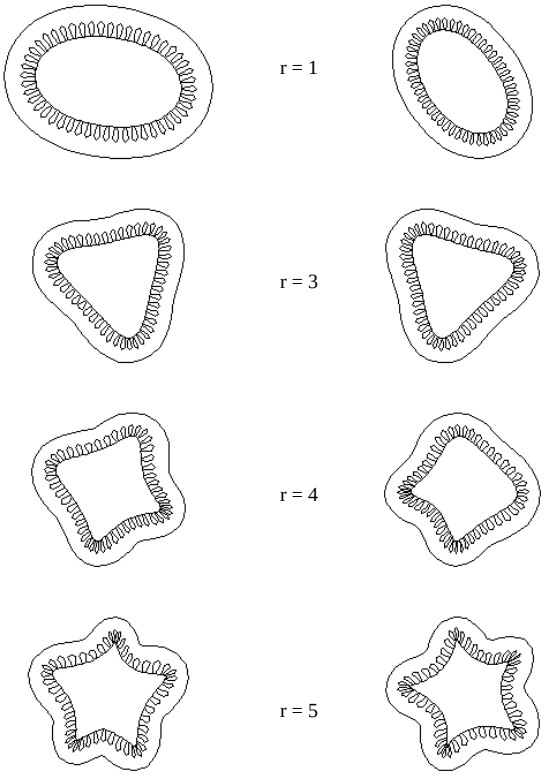

Fig. 4. Various mode shapes of a stator lamination.

The most important excitations for squirrel cage induction machines are the harmonic field waves generated by the stator currents combined with the rotor fields, combined with the harmonics due to the tooth saturation and combined with harmonics due to a rotor eccentricity. Static as well as dynamic eccentricity can be considered. The pole pair numbers and frequencies for particular field combinations can be taken from the literature [1, 2]. With this rather simple model very useful information about the expected noise radiation can be obtained e.g. undesired stator / rotor slot combinations, which can result in audible noise, can be derived from this model. In the industrial practice this model can be easily coded in a computer program. However, only electromagnetic effects are considered. Audible noise caused by magnetostriction is not accounted for in this model. Here the numerical models, e.g. coupled finite element models, are better suited to study such effects.

A. Example Calculation

For a 4-pole 2p=4 induction motor with a stator-slot/rotor-bar ratio of N_1/N_2=48/40 the vibration excitation caused by a particular stator winding field harmonic with pole pair number $\boldsymbol{n}_1 = p(1+6g_1) = -46 \quad (g_1 = 0, \pm 1, \pm 2, \dots)$ and a particular rotor field harmonic $\boldsymbol{n}_2 = p + g_2 N_2 = 42 \quad (g_2 = \pm 1, \pm 2, \dots)$ excited by the fundamental stator field is determined as an example. With this combination a mode shape $r = (\boldsymbol{n}_2 \pm \boldsymbol{n}_1) = 42 - 46 = -4$ is generated (Fig. 4) at a vibration frequency of

$$f_r = f_1 \left\{ \begin{matrix} \frac{g_2 N_2}{p} + \begin{matrix} 2 \text{for } r = n_2 + n_1 \\ 0 \text{for } r = n_2 - n_1 \end{matrix} \end{matrix} \right\} = 50Hz \left\{ \frac{+1 \cdot 40}{2} + 2 \right\} = 1100\,Hz$$

Saturation fields as well as a static rotor eccentricity can deliver this frequency as well. It must be noted, that this is just a brief example to illustrate in which way the single frequencies, excited by the combinations of particular harmonic fields, can be calculated. Figure 5 shows measurements obtained by a narrow-band audible noise analysis [1]. The frequency of 1100Hz can be found back in the measurements of the machine's audible noise.

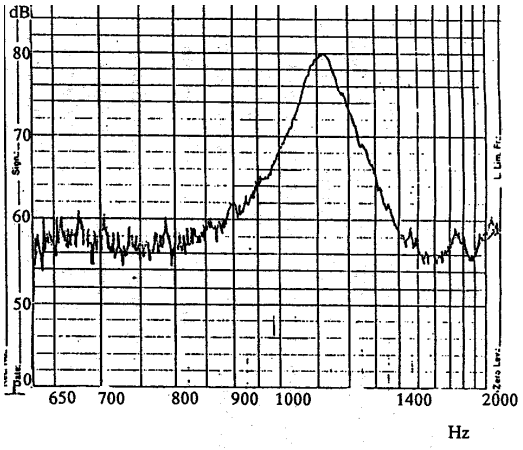

Fig. 5. Narrow-band measurement (without ventilator) of the audible noise of an induction machine at rated load. Motor: 160kW, 380V, 50Hz, 2p=4, N_1/N_2=48/40 (source:[1]).

IV. Numerical Noise Analysis

The main sources of acoustic noise radiated by electric machines are the radial stator vibrations. The numerical study of noise and vibrations of electrical machinery is based upon the coupling between the magnetic field and the mechanical stator deformation. This coupling is usually effected using reluctance forces (Maxwell stress). Since the deformations occurring are small when compared to the machine's dimensions, there is no feedback to the magnetic system. Stator deformations are caused not only by reluctance forces, but also by magnetostriction effects in the stator yoke [7]. Magnetostriction is the main cause of noise for transformers, inductors and other devices without air gap. The magnetostrictive deformations can be calculated based upon the magnetic field and if the deformations are of the same order of magnitude as the deformations caused by the reluctance forces, feedback to the magnetic system must be considered. However, as soon as magnetostriction becomes important, which certainly is the case in actuators based upon the effects of magnetostriction, the magnetic field is affected and the coupling can numerically no longer be implemented without a feedback. Using an iterative solution scheme with the magnetic and mechanical finite element system separated can provide the feedback. In another approach, the two physical systems can be captured in one magneto mechanical matrix, which is solved at once. Next to the magnetisation characteristic of the iron, the magnetostriction characteristic $\lambda(B)$ is required. The term *magnetostriction* relates to this $\lambda(B)$ dependency, while the term *inverse magnetostriction* relates

to the dependency of permeability on mechanical stress. This latter effect is not considered here but was built into a strong numerical coupling in [8].

In order to be able to compute stator deformations, a *local* force expression is required. Here, based upon the coupled magneto mechanical finite element model, a nodal force expression is derived which covers both Lorentz forces and Maxwell stresses on the air-iron interface. The magnetostriction effect is represented by a set of nodal forces giving rise to the same deformation as magnetostriction does.

A. The Magneto Mechanical System With Magnetic Forces

Both magnetostatic and elasticity finite element methods are based upon the minimization of an energy functional. The total energy E of the electromechanical system consists of the *elastic energy* U stored in a body with (small elastic) deformation a [9] and the *magnetic energy* W stored in a linear magnetic system with vector potential A [10]:

$$E = U + W = \frac{1}{2} a^T K a + \frac{1}{2} A^T M A \tag{3}$$

where K is the mechanical stiffness matrix and M is the magnetic 'stiffness' matrix. Considering the similar form of these energy terms, the following system of equations represents the numerically coupled magneto mechanical system:

$$\begin{bmatrix} M & D \\ C & K \end{bmatrix} \begin{bmatrix} A \\ a \end{bmatrix} = \begin{bmatrix} T \\ R \end{bmatrix} \tag{4}$$

where T is the magnetic source term vector and R represents external forces other than those of electromagnetic origin. Setting the partial derivatives of the total energy E with respect to the unknowns $[A\ a]^{\mathrm{T}}$ to zero, the combined system (2) with T=0, R=0 is retrieved:

$$\frac{\partial E}{\partial A} = M A + \frac{1}{2} a^T \frac{\partial K(A)}{\partial A} a = 0 \quad , \tag{5}$$

$$\frac{\partial E}{\partial a} = K a + \frac{1}{2} A^T \frac{\partial M(a)}{\partial a} A = 0 \quad , \tag{6}$$

giving the coupling terms C and D. The coupling term D can be used to represent magnetostriction effects in a numerically *strong* coupled analysis [11], but will not be considered here, so that D=0 and T=MA (magnetostriction will be introduced further on in a numerically *weak* coupling approach). Rearranging the mechanical equation (6) into:

$$K a = -\frac{1}{2} A^T \frac{\partial M(a)}{\partial a} A = -CA = F_{mag}, \tag{7}$$

reveals a means to calculate the forces F_{mag} internal to the magneto mechanical system. These magnetic forces are computed from vector potential A and the *partial derivative* of the magnetic stiffness matrix M with respect to deformation a. This procedure to obtain the magnetic forces F_{mag} is equivalent to applying the virtual work principle to the magnetic energy W for a virtual displacement a:

$$F_{mag} = -\frac{\partial W}{\partial a} = -\frac{\partial}{\partial a}\left[\frac{1}{2} A^T M(a) A\right], \tag{8}$$

where vector potential A has to remain unchanged (constant flux). For the non-linear case, the matrix M is a function of the magnetic field and displacement: $M(A,a)$. The magnetic energy W is now given by the integral

$$W = \int_0^A T^{\mathrm{T}}\, dA = \int_0^A A^T M\, dA\,, \tag{9}$$

where T=MA and M^{T}=M was used. The force expression (8) now becomes

$$F_{mag} = -\frac{\partial W}{\partial a} = -\int_0^A A^{\mathrm{T}} \frac{\partial M(A,a)}{\partial a} dA\,. \tag{10}$$

Note that adding a constant to A indeed does not change the value of the integrals in (9) and (10). For D=0, the initial coupled system (4) can therefore be rearranged into the decoupled system:

$$\begin{bmatrix} M & 0 \\ 0 & K \end{bmatrix} \begin{bmatrix} A \\ a \end{bmatrix} = \begin{bmatrix} T \\ R + F_{mag} \end{bmatrix}, \tag{11}$$

and solved in a numerically weak coupled cascade scheme.

B. Magnetostriction Forces

Effects with a mutual influence between the mechanical deformation or stress and the magnetisation $\mu_0 M$ in the material, are called *magneto mechanical effects*. The most important is the *magnetostriction effect* $\lambda(B)$, pertaining to the strain λ of a piece of material due to its magnetisation. The *inverse magnetostriction* effect is the dependency of the magnetisation $\mu_0 M$ on the stresses σ occurring in the material. Since stress influences magnetisation, it will also influence the magnetostriction itself and turn the $\lambda(B)$ characteristic into a $\lambda(B,\sigma)$ dependency [12]. Usually there is no relevant volume change due to magnetostriction [13]. Typical material characteristics are plotted in Fig. 6.

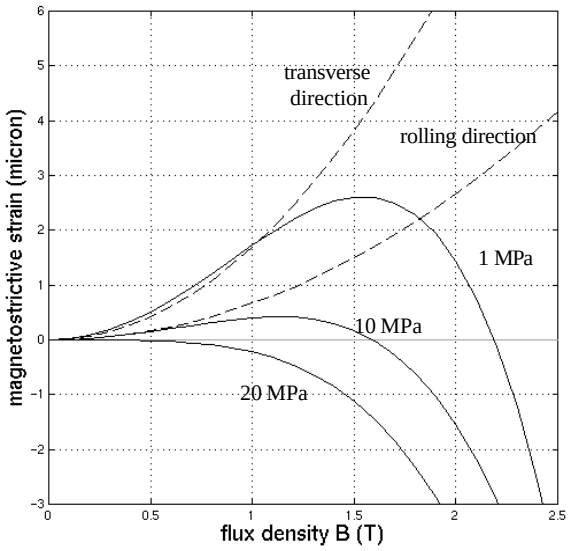

Fig. 6. Magnetostrictive material characteristics of non-oriented 3% SiFe (solid lines, as a function of tensile stress) and M330-50A (dashed lines, for rolling and transverse direction).

Magnetostriction is implemented in the coupled system by a force distribution F_{ms} , which is added to R and F_{mag} in (11).

$$\begin{bmatrix} M & 0 \\ 0 & K \end{bmatrix} \begin{bmatrix} A \\ a \end{bmatrix} = \begin{bmatrix} T \\ R + F_{mag} + F_{ms} \end{bmatrix} \tag{12}$$

By *magnetostriction forces* we indicate the set of forces that induces the same strain in the material as magnetostriction does. This approach is similar to how thermal stresses are usually taken into account [14]. To evaluate thermal stresses, the thermal expansion of the free body (no boundary conditions) is calculated based upon the temperature distribution, and then the thermal stresses are found by deforming the expanded body back into its original shape (back inside the original boundary conditions). To calculate magnetostriction forces, the expansion of the free body due to magnetostriction is found based upon the magnetic flux density, and the magnetostriction forces are found as the reaction to the forces needed to deform the expanded body back into the original boundary conditions.

For finite element models, this can be performed on an element by element basis, where the midpoint of the element (the centre of gravity) can be used as a locally fixed point. The magnetostrictive deformation of the element, i.e. the displacement of the three nodes with respect to the midpoint, is found using the element's flux density B^e and the $\lambda(B)$ characteristic of the material (Fig. 5). Fig.6a shows the original element (solid line) and the deformed element (dashed line) after applying the magnetostrictive strain $\lambda(B^e)$ keeping the centre fixed. The magnetostriction forces F_{ms} (Fig.6b) are the set of forces inducing the same deformation.

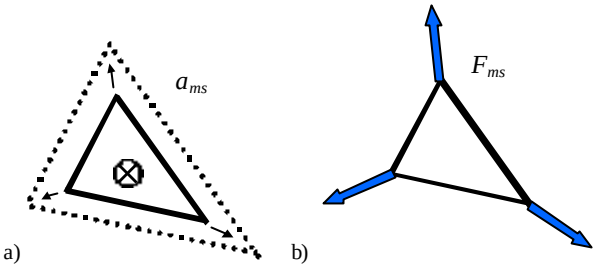

Fig. 6. The center of gravity of the element is considered to be fixed while the magnetostrictive expansion $\lambda(B^e)$ is applied to the nodes. This deformation is represented by a set of mechanical forces $F_{ms.}$

It must be noted that due to the fact that magnetostriction usually leaves the volume unchanged, the magnetostrictive 'Poisson modulus' for the material studied e.g. ν_{ms}=0.5, while the mechanical Poisson modulus of this material is about ν=0.3. This means that, next to a set of forces *parallel* to **B**, there will always be a set of forces *perpendicular* to **B** (Fig.7).

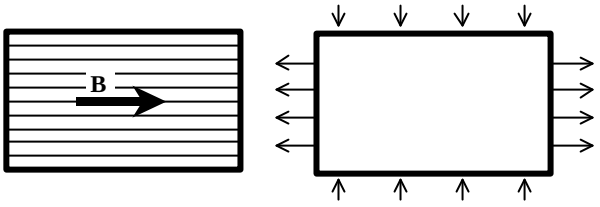

Fig. 7. The set of forces (right) representing the strain caused by magnetostriction due to the magnetic field **B** (left), consists of a set forces parallel to **B** and a set forces perpendicular to **B**.

C. Example: 6-pole Synchronous Machine

Fig.8 shows the magnetic field in one pole of a six-pole synchronous machine. B_{max} in the teeth is 1.26 T corresponding to λ = 2.3 μm/m for 3% SiFe with 1 MPa tensile stress. Fig.9 shows the magnetostriction forces on the stator for the magnetic field of the motor. Isotropic material properties can be considered with this model as well. Fig.9a illustrates the simulations for a stator of isotropic non-oriented 3% SiFe and Fig.9b for a stator of anisotropic M330-50A (both materials were modelled with Young modulus E= 2.2 10^{11} Pa and ν = 0.3). In the areas of high flux density in the stator, there are magnetostriction forces parallel to the flux lines and also a set of magnetostriction forces perpendicular to the flux lines, both seeking to *increase* the circumference of the stator. In the anisotropic case, the general magnetostriction force pattern remains the same, but the forces appear slanted. Fig.10 repeats Fig.9a but also shows the magnetic reluctance forces F_{mag} for the magnetic field computed in Fig.8. It can be seen that F_{ms} and F_{mag} are of the same order of magnitude (the size of the nodal force vectors on the teeth tips is 25 N).

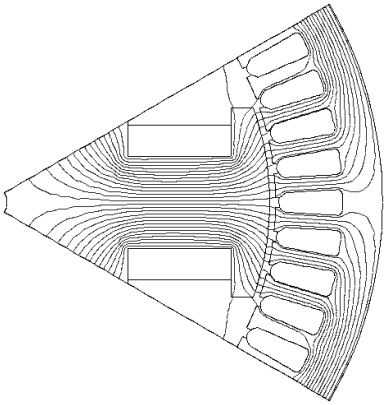

Fig. 8. Magnetic flux lines in one pole of a 6-pole synchronous machine.

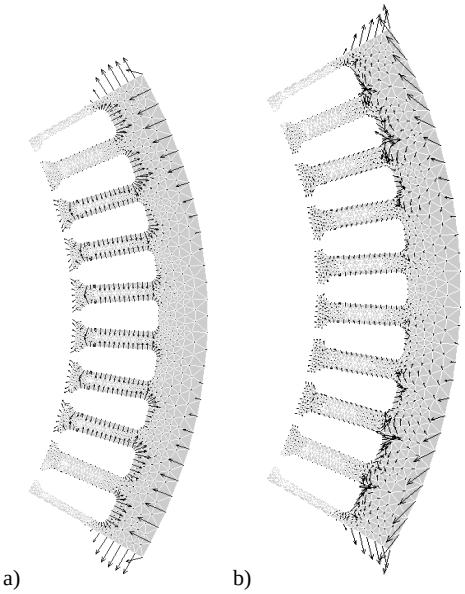

a) b)

Fig.9 Magnetostriction forces on stator for a) isotropic non-oriented 3% SiFe and b) anisotropic M330-50A.

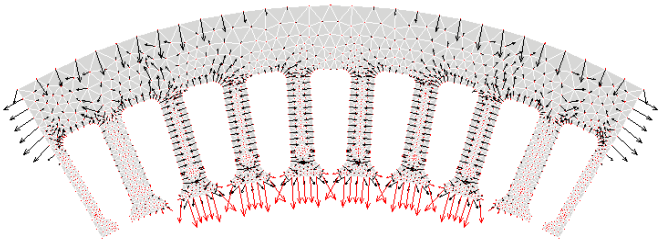

Fig.10 Comparison between reluctance forces (on the teeth tips) and magnetostriction forces (on the stator surface).

VI. CONCLUSIONS

The analysis of audible noise excited by electrical machinery can be performed both, by analytical and by numerical models. In spite of various rigorous assumptions in this model, it is possible to predict the narrow-band audible noise of magnetically excited vibrations of an induction machine.

In the coupled numerical model the mechanical and magnetic finite element system are combined into one magneto mechanical system. This results in a finite element based expression for nodal forces representing both Lorentz forces and reluctance forces (Maxwell stresses on material interfaces), for both linear and nonlinear materials. The magnetostriction of the material is taken into account by a force distribution (magnetostriction forces) that induces the same strain into the material as magnetostriction does. This is done for both isotropic and anisotropic materials. These force distributions can be added to other force distributions to start a subsequent mechanical deformation or vibration analysis.

REFERENCES

[1] Seinsch, H. O., *Oberfelderscheinungen in Drehfeldmaschinen*, Teubner, Stuttgart, 1992.

[2] Jordan, H., *Geräuscharme Elektromotoren*, W.Girardet, Essen, 1950.

[3] Ramesohl, I., *Numerische Geräuschberechnung von Drehstrom-Klauenpolgeneratoren*, PhD RWTH Aachen, 1999.

[4] Bauer, Th., *Elektromagnetische, strukturdynamische und akustische Berechnung und Optimierung von Induktionstiegelöfen*, PhD RWTH Aachen, 2000.

[5] Arians, Guido, *Numerische Berechnung der elektromagnetischen Feldverteilung, der strukturdynamischen Eigenschaften und der Geräusche von Asynchronmaschinen*, PhD RWTH Aachen, Shaker Verlag, 2001.

[6] Delaere, Koen, *Computational and experimental Analysis of electrical machine vibrations caused by magnetic forces and magnetostriction*, PhD KULeuven, 2002.

[7] Laftman, L., *Contribution to Noise from Magnetostriction and PWM Inverter in an Induction Machine*, Ph.D. thesis, Dept. of Industrial Electrical Eng. and Automation, Lund Institute of Technology, KF Sigma, Sweden 1995.

[8] Besbes, M., Ren, Z., Razek, A., "Finite Element Analysis of Magneto-Mechanical Coupled Phenomena in Magnetostrictive Materials", *IEEE Transactions on Magnetics*, Vol.32, no.3, May 1996, pp.1058-1061.

[9] Zienkiewicz, O.C., Taylor, R.L. (1989), *The Finite Element Method*, McGraw-Hill.

[10] Silvester, P.P., Ferrari R.L. (1996), *Finite Elements for Electrical Engineers*, Third Edition, Cambridge University Press.

[11] Delaere, K., Belmans, R., Hameyer, K, "Introducing magneto-striction into magnetomechanical analysis," *Proc. Conf. Intern. Conf. on Electric Machines ICEM 2000*, Finland, 28-30 August, 2000.

[12] Jiles, D., *Introduction to Magnetism and Magnetic Materials*, Chapman & Hall, 1991.

[13] Cullity, B.D., *Introduction to Magnetic Materials*, Addison-Wesley (Series in Metallurgy and Materials), Philippines, 1972.

[14] Hirsinger, L., *Etude des deformations magneto-elastiques dans les materiaux ferromagnetiques doux. Application a l'etude des deformations d'une structure de machine electriques*, PhD, Laboratoire de Mecanique et Technologie, Universite Paris 6, 1994.